Biofilter Media Gas Pressure Loss as Related to Media Particle Size and Particle Shape

Lorenzo Pugliese[1]; Tjalfe G. Poulsen[2]; and Rune R. Andreasen[3]

Abstract: Pressure loss (ΔP) is a key parameter for estimating biofilter energy consumption. Accurate predictions of ΔP as a function of air velocity (V) are, therefore, essential to assess energy consumption and minimize operation costs. This paper investigates the combined impact of medium particle size and shape on the V-ΔP relationship. The V-ΔP measurements were performed using three commercially available materials with different particle shapes: crushed granite (very angular particles), gravel (particles of intermediate roundness), and lightweight clay aggregrate (almost spherical particles). A total of 21 different particle-size fractions, with particle sizes ranging from 2 to 14 mm, were considered for each material. As expected, ΔP decreased with increasing particle size in agreement with earlier findings. The value of ΔP, however, also showed a tendency to decrease with increasing particle roundness especially for fractions containing smaller particles. A new model concept for estimating V-ΔP across different particle-size fractions and shapes was proposed. This model yielded improved prediction accuracy in comparison with existing prediction approaches. **DOI: 10.1061/(ASCE)EE.1943-7870.0000771.**

CE Database subject headings: Air flow; Granular media; Permeability; Particle size distribution; Moisture; Filtration.

Author keywords: Air flow; Granular media; Permeability; Pressure loss; Particle-size distribution; Particle shape; Moisture; Filtration.

Introduction

Biofiltration is one of the most widely employed technologies for removal of organic pollutants (including malodorous compounds) in air streams originating from industrial and commercial activities (Goldstein 1996; Nicolai and Janni 2000). The filtration process is carried out by the use of microorganisms that are immobilized in a biofilm attached to a porous packing (carrier) material such as straw, wood chips, pebbles, or various artificial materials. Removal of the contaminants then occurs as a consequence of the microbial metabolism where the contaminants are degraded to yield carbon and energy for microbial growth. Biofiltration cost efficiency is generally defined as the quantity of air cleaned to a required level per amount of operation costs. Filter cleaning capacity depends on the quantity of active biomass in the filter, which in turn depends on the active specific surface of the packing material. Operation costs are for a large part connected with the energy consumption of the filter, which in turn is mainly associated with the pressure loss across the filter. Thus material physical properties, such as specific surface area and airflow resistance, are key parameters to consider when assessing biofilter performance (Wani et al. 1997; McNevin and Barford 1998; Kim et al. 2000; Elias et al. 2003; Barona et al. 2004). By choosing a proper porous medium, it is possible to increase active microbial biomass (De Oliveira et al. 2009) and contaminant removal capacity (Sakuma et al. 2006) and to reduce the energy consumption associated with the airflow resistance of the biofilter (Malhautier et al. 2005; Gadal-Mawart et al. 2010).

Filter pressure loss (ΔP) is a key parameter for estimating biofilter energy consumption. Accurate predictions of ΔP are, therefore, necessary when designing biofilters, selecting biofilter packing materials, and estimating economic costs. Darcy (1856) proposed a linear expression relating ΔP with packing material properties (permeability) based on studies of water flow in filter sand. Several studies have subsequently investigated the relationship between permeability, particle size, and porosity for porous media (Kozeny 1927; Fair and Hatch 1933; Carman 1937; Scheidegger 1960; Sorrentino and Anlauf 1999; Sperl and Trckova 2008; Hamamoto et al. 2009).

Forchheimer (1901) observed that in porous media at high fluid flow velocity (V), the relationship between V and ΔP was not linear as predicted by Darcy's law but instead followed a second-order relationship. Therefore a quadratic V term was added to the Darcy equation to take the effects of inertial forces and turbulence into account. Ergun (1952) proposed a Forchheimer-based expression that essentially links the ΔP to fluid-filled porosity (ε), a medium particle specific characteristic length (D_{eq}) and a set of empirical constants that were supposed to be universal across different porous materials. Ahmed and Sunada (1969) proposed a rearrangement of the Forchheimer equation using the Navier-Stokes equations. The new relationship showed that the empirical constants were related to the properties of the fluid and the porous media by the intrinsic permeability and a proportionality factor (Chin et al. 2009). Ward (1966) derived the same equation by using a dimensional analysis.

Macdonald et al. (1979) evaluated the accuracy of the Ergun equation. A large number of experimental data from different porous media were used. The results of Macdonald et al. (1979) showed that the empirical constants in the equation were not independent of porous medium properties, thus, complicating the use of

[1]Ph.D. Student, Dept. of Chemistry and Biotechnology, Aalborg Univ., Sohngaardsholmsvej 57, Alborg DK-9000, Denmark (corresponding author). E-mail: lp@bio.aau.dk

[2]Associate Professor, Dept. of Chemistry and Biotechnology, Aalborg Univ., Sohngaardsholmsvej 57, Aarhus DK-9000, Denmark. E-mail: tgp@bio.aau.dk

[3]Postdoctoral Researcher, Dept. of Agroecology, Aarhus Univ., Blichers Allé 20, Aarhus DK-8830, Denmark. E-mail: RuneR.Andreasen@agrsci.dk

Note. This manuscript was submitted on March 20, 2013; approved on August 10, 2013; published online on August 13, 2013. Discussion period open until May 1, 2014; separate discussions must be submitted for individual papers. This paper is part of the ***Journal of Environmental Engineering***, Vol. 139, No. 12, December 1, 2013. © ASCE, ISSN 0733-9372/2013/12-1424-1431/$25.00.

the Ergun equation across different types of porous media. Trussell and Chang (1999) analyzed the validity of the Forchheimer and the derived relations on a large set of data (glass beads, anthracite, sand, potter's beads, marbles, and fragments of crushed dolerite) with respect to impact of medium particle size on ΔP. The results pointed out difficulties in determination of the empirical model parameters, thus, leading to prediction errors. Andreasen and Poulsen (2013) investigated ΔP in a set of coarse-grained porous materials (with a particle diameter greater than or equal to 2 mm) relevant for biofiltration and found that ΔP was only weakly dependent on air-filled porosity (ε) for this type of media. These authors, therefore, proposed a simplified model concept for predicting ΔP based on particle-size distribution and particle diameter rather than on material air-filled porosity as traditionally done. The model, developed and tested using a set of media with a wide range of particle sizes, yielded predictions equivalent to 90% reduction in prediction error compared to the Ergun equation. The media tested, however, all belonged to the same material [Leca (Weber A/S, Denmark), a granular material used for insulation and biofiltration consisting of porous rounded particles] and there is thus, a need to verify if this model concept is applicable for others types of porous materials, including materials with different particle shapes.

Particle shape influences many physical properties of porous materials such as void ratio, internal friction angle, and air permeability (Witt and Brauns 1983; Shinohara et al. 2000; Rouse et al. 2008). Studies by Connell et al. (1999), Endo et al. (2001), and Pugliese et al. (2012) indicate that particle shape does have an impact on the V-$\Delta P/L$ relationship, although at present very little is known about how particle shape affects ΔP in porous media.

The aim of this study is, therefore, to investigate the effects of particle shape on the V-$\Delta P/L$ relationship across porous materials with different particle shapes and particle-size distributions relevant for biofiltration. The investigation will be based on measurement of ΔP in three different commercially available granular materials, which have very different particle shapes: crushed granite (very angular particles), gravel (particles of intermediate roundness), and Leca (almost spherical particles). A total of 21 different particle-size fractions, with particle sizes ranging from 2 to 14 mm were considered for each of the three materials.

Theory

At low V, the ΔP of a fluid flowing through a porous medium can be described by Darcy's law (Darcy 1856) which, however, is only valid for Reynolds numbers (R) (Andreasen et al. 2012) below approximately 1, when flow conditions are laminar and the inertial forces in the flow field are negligible. At R greater than 1 (higher flow V), inertial forces are important, the V-ΔP relationship becomes nonlinear and Darcy's law no longer applies. Several nonlinear equations for relating V and ΔP in this region of R have been presented (Green and Duwez 1951; Cornell and Katz 1953; Geertsma 1974; Antohe et al. 1997; Lage et al. 1997; Trussell and Chang 1999) but the most widely used is the second-order Forchheimer relationship (Forchheimer 1901). This relationship was originally developed for $1 < \mathrm{R} < 100$, but it can also be used to approximate the V-ΔP relationship above $\mathrm{R} = 100$ (Trussell and Chang 1999; Andreasen and Poulsen 2013).

Among the expressions describing fluid flow through packed beds following the Forchheimer relationship, the Ergun equation (Ergun 1952) is perhaps the most widely used. This equation uses an equivalent particle diameter (D_{eq}) and three empirical constants for which Ergun suggested universal values. Macdonald et al. (1979) later tested the Ergun equation against a large set of flow-pressure data from several porous media and found that the empirical constants depended on the physical properties of the media. Macdonald et al. (1991) proposed an expression for estimating D_{eq}, using the first- and the second-order moments of the particle-size distribution. A more thorough presentation of the preceding theory and the equations involved can be found in Andreasen et al. (2012), Andreasen and Poulsen (2013), and Andreasen et al. (2013).

A simpler expression to evaluate D_{eq} was proposed by Andreasen and Poulsen (2013). Based on measurements for a large set of porous media with uniform particle-size distributions originating from the same material (Leca, with diameters ranging from 2 to 18 mm) D_{eq}, for materials with uniform particle-size distributions, was estimated as a harmonic mean of the mean particle diameter (D_m) and the minimum particle diameter (D_{min}) for each medium as

$$D_{\mathrm{eq}} = \frac{2}{\frac{1}{D_m} + \frac{1}{D_{\mathrm{min}}}} \tag{1}$$

Andreasen and Poulsen (2013) further observed that ΔP in these media was almost independent of air-filled porosity and therefore suggested that ΔP can be predicted as

$$\frac{\Delta P}{L} = A\left(\frac{2}{\frac{1}{D_m} + \frac{1}{D_{\mathrm{min}}}}\right)^{-2} \mu V + B\left(\frac{2}{\frac{1}{D_m} + \frac{1}{D_{\mathrm{min}}}}\right)^{-1} \rho V^2 \tag{2}$$

where ΔP = the pressure drop across the medium (Pa); L = the distance over which the pressure drop takes place (m); μ = the air viscosity (Pa s); ρ = the air density (kg/ m^3); V = the superficial air velocity (m/s); and A and B = empirical constants. Based on this study, the authors concluded that a likely dependency of $\Delta P/L$ on particle shape was expected. The authors also suggested that instead of defining D_{eq} based on the smallest and largest particle diameter, improved predictions might be achieved by using alternative values.

Particle shape is often characterized by particle roundness, which is the ratio between the diameters of the largest inscribed and the smallest circumscribing spheres (Santamarina and Cho 2004). Earlier studies (Krumbein 1941; Meloy 1977; Barret 1980; Bowman et al. 2001) have concluded that the projection sphericity (equivalent to roundness) (Cox 1927; Pentland 1927; Tickell 1931; Wadell 1935) represents the best way to analyze effects of particle shape on transport in porous media. Two very widely applied approaches are those of Pentland (1927) and Wadell (1935). Pentland (1927) defined the roundness as

$$\varphi_p = \frac{\omega}{\omega_p} \tag{3}$$

where φ_p = the total degree of roundness (dimensionless) based on Pentland (1927) which cannot be greater than 1; ω = the cross-sectional or projection area of the grain (m^2); and ω_p = the area of the circle having the largest diameter of the grain (m^2). The orientation of the particles was not definite.

Wadell (1935) defined the roundness as

$$\varphi_w = \frac{N}{\sum_N \left(\frac{\mathcal{R}}{r_N}\right)} \tag{4}$$

where φ_w = the total degree of roundness based on Wadell (1935) (dimensionless); N = the number of corners in the given plane of the particle; $\mathcal{R}$ = the radius of the largest inscribed circle (m); and r_N = the radius of the inscribed circle of the Nth corner of the particle in the plane (m).

Materials and Methods

Measurements of ΔP were conducted using three commercially available materials: crushed granite, gravel, and Leca (light expanded clay aggregates). An irregular and very angular particle shape characterizes the crushed granite; gravel consists of somewhat rounded rock fragments and Leca consists of rounded particles. Granite and gravel do not have any internal porosity (inside the particles) while Leca consists of highly porous particles; although this internal porosity is inaccessible by air as it consists of closed vesicles very much like soap foam. Fig. 1 shows the three materials.

All three materials were initially sieved into six particle-size fractions with uniform particle-size distributions. Each of these fractions was characterized by a particle-size range (R) of 2 mm in the range between 2 and 14 mm. Particle diameters (D) were $2 \le D < 4$, $4 \le D < 6$, $6 \le D < 8$, $8 \le D < 10$, $10 \le D < 12$, and $12 \le D < 14$ mm corresponding to mean particle diameter (D_m) of 3, 5, 7, 9, 11, and 13 mm, respectively. Additional fractions with $R = 4$ mm ($D_m = 4, 6, 8, 10, 12$ mm); $R = 6$ mm ($D_m = 5, 7, 9, 11$ mm); $R = 8$ mm ($D_m = 6, 8, 10$); $R = 10$ mm ($D_m = 7, 9$); and $R = 12$ mm ($D_m = 8$), with uniform particle distributions, were produced by combining appropriate quantities of the six $R = 2$ mm fractions. Uniform particle-size distributions were chosen to ensure well-defined particle-size distributions across all particle-size fractions used. A total of 63 particle-size fractions were produced (21 for each material).

For granite, ρ_b for each particle size fraction was measured by packing the material into a known volume followed by weighing. The external porosity (ε_{ex}), which for granite equals ε_{tot}, was calculated from ρ_b using a solid density of 2.75 g/cm^3 (Hausrath et al. 2009; Omosanya et al. 2012). Corresponding values of ρ_b and $\varepsilon_{ex}(\varepsilon_{tot})$ for gravel and Leca were obtained from Sharma and Poulsen (2010) and Andreasen and Poulsen (2013), respectively. For determination of roundness, φ_p and φ_w, 30 particles were randomly selected from each of the 3 materials (5 particles for each of the 6 $R = 2$ mm fractions). For all granite and gravel particles, projections of particle shape onto a flat surface were carried out in three perpendicular planes. For Leca, projections were only carried out in one plane as particle shape was observed to be very similar in all planes. Values of ω and ω_p, and consequently φ_p [Eq. (3)] were subsequently determined from the projections. Values of $\mathcal{R}$ and r_N and consequently φ_w [Eq. (4)] were determined by selecting the two sharpest corners of each projection ($N = 2$) and analyzed using a circle scale as proposed by Wadell (1935). Average values of φ_p and φ_w were then calculated for each material across the 6 $R = 2$ mm particle-size fractions (five particles for each). All measurements were carried out in duplicate. An overview of the media properties is given in Table 1.

Each experiment was performed by packing each of the 21 particle-size fractions for each of the 3 materials into a clear acrylic column of 100 cm in length and 14 cm inner diameter. This column size was chosen in order to avoid effects of preferential flow along the column walls, which may occur if column diameter is too small, compared to the average particle diameter (Pugliese et al. 2012). Great care was taken to achieve a uniform packing (especially along the length of the column), to reduce variations in ρ_b. Measurements of ΔP were carried out for each of the 63 particle size fractions following the approach of Pugliese et al. (2012). Columns were fitted with a polyethylene lid and sealed with a rubber O-ring at the bottom. A stainless steel mesh with 2-mm openings and 1-mm thickness was installed to maintain a distance of 10 mm between the lid and the porous medium. The top of the column was kept open to the atmosphere while the bottom was connected to a supply of compressed atmospheric air via a valve and a precision ball flowmeter (Model P450) (Porter Instrument Div., Hatfield, PA). Soft Teflon tubing with an inner diameter of 4 mm was used to connect system components. Corresponding values of V and ΔP across the columns were measured for $V = 0.005$, 0.010, 0.016, 0.021, 0.032, 0.043, 0.054, and 0.065 m/s, equal to $Q = 5$, 10, 15, 20, 30, 40, 50, and 60 l/min, respectively. The relatively wide Q-range was chosen to get more reliable determination of the V-ΔP relationships for the different media. An Alnor AXD 560 digital manometer (Alnor, Ontario, Canada), connected to the bottom and the top of the column, was used to measure ΔP. Measured ΔP values were corrected for the pressure drop across the empty column with the metal mesh in place. All experiments were carried out in duplicate. A schematic of the experimental setup is shown in Fig. 2.

Results and Discussion

Measured V-$\Delta P/L$ relationships for selected particle-size fractions for all three materials are shown in Fig. 3.

Fig. 1. Porous materials used in the tracer experiments: (a) granite; (b) gravel; (c) Leca

Table 1. Physical Properties of the Three Porous Materials (Granite, Gravel, and Leca) and 63 Particle-Size Fractions

	Granite			Gravel			Leca		
	ρ_p (g/cm^3)	φ_p	φ_W	ρ_p (g/cm^3)	φ_p	φ_W	ρ_p (g/cm^3)	φ_p	φ_W
Size range	2.75	0.64	0.09	2.65	0.65	0.51	0.40	0.80	0.89
(mm)	ρ_b (g/cm^3)	$\varepsilon_{tot} = \varepsilon_{ex}$ (cm^3/cm^3)		ρ_b (g/cm^3)	$\varepsilon_{tot} = \varepsilon_{ex}$ (cm^3/cm^3)		ρ_b (g/cm^3)	ε_{ex} (cm^3/cm^3)	ε_{tot} (cm^3/cm^3)
2–4	1.51	0.45		1.55	0.42		0.33	0.28	0.88
4–6	1.55	0.44		1.54	0.42		0.29	0.39	0.89
6–8	1.52	0.45		1.54	0.42		0.25	0.37	0.91
8–10	1.48	0.46		1.55	0.41		0.25	0.37	0.91
10–12	1.46	0.47		1.55	0.41		0.24	0.36	0.91
12–14	1.47	0.47		1.55	0.41		0.23	0.33	0.91
2–6	1.53	0.44		1.54	0.42		0.31	0.33	0.88
4–8	1.50	0.45		1.53	0.42		0.27	0.37	0.90
6–10	1.53	0.44		1.54	0.42		0.25	0.37	0.91
8–12	1.49	0.46		1.56	0.41		0.24	0.37	0.91
10–14	1.46	0.47		1.55	0.42		0.24	0.35	0.91
2–8	1.55	0.44		1.56	0.41		0.29	0.34	0.89
4–10	1.50	0.45		1.54	0.42		0.26	0.37	0.90
6–12	1.48	0.46		1.55	0.42		0.24	0.37	0.91
8–14	1.49	0.46		1.56	0.41		0.24	0.34	0.91
2–10	1.54	0.44		1.59	0.40		0.27	0.36	0.90
4–12	1.52	0.45		1.58	0.41		0.26	0.37	0.90
6–14	1.52	0.45		1.56	0.41		0.24	0.35	0.91
2–12	1.55	0.44		1.58	0.40		0.27	0.35	0.90
4–14	1.53	0.44		1.59	0.40		0.25	0.36	0.91
2–14	1.54	0.44		1.61	0.39		0.26	0.35	0.90

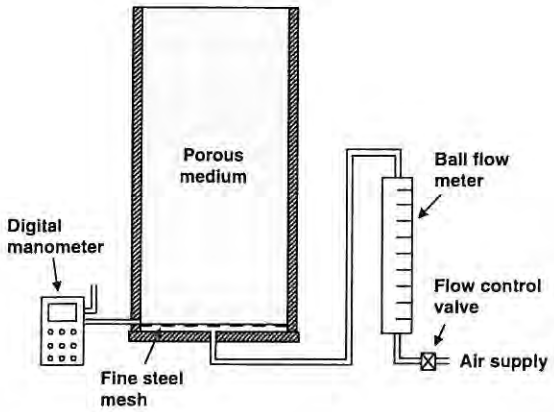

Fig. 2. Experimental setup for measuring pressure loss (ΔP) in porous filter media

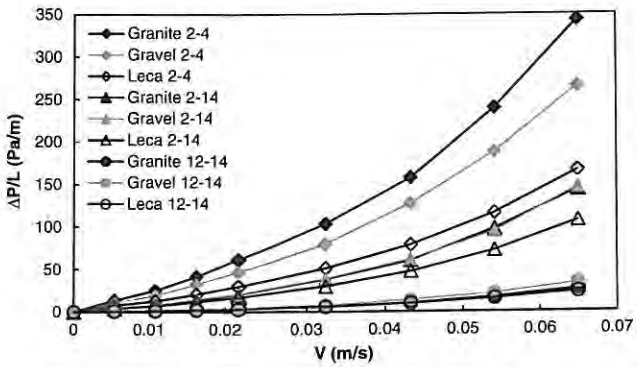

Fig. 3. Measured values of $\Delta P/L$ as a function of V for three selected fractions (2–4, 2–14, 12–14 mm) for the three materials (granite, gravel, Leca) considered in this study

The V-$\Delta P/L$ relationships follow a second-order polynomial in all cases, thus, being consisted with Eq. (2). This was the case for all materials and particle-size fractions investigated. Values of R range up to 60, covering therefore both the Darcy and Forchheimer flow domains. $\Delta P/L$ generally decreased with increasing average particle size. The reason is that smaller particles means smaller pores and, thus, increasing resistance to flow. The smallest pores of the media considered here characterize the 2–4 mm fractions (average particle size equal to 3 mm) and, therefore, this medium has the greatest ΔP. In contrast, the lowest values of $\Delta P/L$ were obtained for the 12–14 mm particle size fraction that has the largest average particle diameter (13 mm) and, therefore, also the largest pores.

For identical particle-size fractions, the crushed granite generally yielded the highest $\Delta P/L$ while Leca yielded the lowest values of $\Delta P/L$ despite the fact that granite has a higher external (active) air-filled porosity compared to Leca (Table 1). In fact, for the three materials considered in this study, $\Delta P/L$ was inversely correlated with active air-filled porosity. This supports the findings of Andreasen and Poulsen (2013) who observed that $\Delta P/L$ was independent of active air-filled porosity across a wide range of Leca particle-size fractions. These authors, therefore, suggested to base models for predicting $\Delta P/L$ in coarse-grained (2–18 mm) granular materials on particle diameter rather than air-filled porosity. This is likely because active porosity in fine-grained materials (less than 2 mm) for which Eq. (2) was originally developed, has a very different structure due to for instance cracks and formation of aggregates compared to coarse-grained materials such as those investigated here. Gravel exhibited intermediate ΔP compared to Leca

and crushed granite. The granite and gravel $\Delta P/L$ were 1.24 and 1.19 times larger than those for the Leca on average across all particle-size fractions, respectively. In general, the relative differences in $\Delta P/L$ between the three materials were most prominent for the fractions containing smaller particles.

Values of particle roundness for the three materials as calculated by Pentland (1927) [Eq. (3)] and Wadell (1935) [Eq. (4)] were lowest for granite and highest for Leca. As the principal difference between the three materials considered here is their particle shape (as characterized by roundness), the deviations in ε_{ex} and ρ_b, and $\Delta P/L$ between the three materials likely result from the differences in roundness. Flow in materials consisting of rounded particles (Leca) should be expected to be more laminar and less subject to inertial forces than flow in materials consisting of more angular (less spherical) particles such as crushed granite. Pugliese et al. (2012) observed that, in two materials with identical particle-size distributions but different particle shapes (pebbles with high roundness and crushed slate with low roundness), dispersivity decreased with decreasing particle roundness. This behavior was therefore attributed to the difference in particle shape. The same authors further observed an inverse linear proportionality between dispersivity and $\Delta P/L$ under otherwise identical conditions. Thus $\Delta P/L$ was observed to increase with decreasing particle roundness supporting that the differences in $\Delta P/L$ observed between the three materials used here mainly stems from differences in particle shape. In general the results discussed earlier show that among the three factors (particle size, particle shape, and porosity) particle size is the most important for controlling $\Delta P/L$ (a well-known fact) followed by particle shape, while porosity has little or no impact on $\Delta P/L$ in coarse-granular materials.

The model [Eq. (2)], suggested by Andreasen and Poulsen (2013) for predicting the V-$\Delta P/L$ relationships in materials with uniform particle-size distributions (developed based on data for 36 Leca particle-size fractions), was tested against the V-$\Delta P/L$ values measured in this study for all three materials (1,008 data points). The test was performed by fitting Eq. (2) to the measured data using the model constants A and B as fitting parameters. Optimal values of A and B for each of the three materials were identified by minimizing the sum of the relative squared errors (RSE) between measured and fitted ΔP values, calculated as

$$\mathrm{RSE} = \sum_{i=1}^{N} \left[\frac{\Delta P/L_{\mathrm{measured}}(i) - \Delta P/L_{\mathrm{predicted}}(i)}{\Delta P/L_{\mathrm{measured}}(i)} \right]^2 \quad (5)$$

where $\Delta P/L_{\mathrm{measured}}$ (i) and $\Delta P/L_{\mathrm{predicted}}$ (i) = the observed and predicted (by the model) pressure gradients, respectively; while N = the total number of measurements.

The optimal values of A and B for the three materials are given in Table 2 and the fitted versus measured values of $\Delta P/L$ by Eq. (2) with the A and B values from Table 2 are shown in Fig. 4 for the three materials.

Values of A and B for Eq. (2) are relatively similar across the three materials with averages of 443 (±9%) and 56 (±15%), respectively, with numbers in parentheses indicating one standard deviation. In general the model is able to fit the data relatively well with relative RSE values ranging from 0.17 to 0.21 indicating that the average squared error in fitting individual values of $\Delta P/L$ is 0.19 on average.

Fig. 4 shows that it is possible to get a relatively close fit of Eq. (2) to the measured $\Delta P/L$ values especially considering that the $\Delta P/L$ varies over three orders of magnitude. The plots, however, also show that Eq. (2) has a tendency to underpredict small $[-0.5 < \log(\Delta P/L) < 0.5]$ and large $[2.0 < \log(\Delta P/L) < 2.5]$ $\Delta P/L$ values. This behavior is actually not seen only for the three data sets as a whole but also for the individual particle-size fractions for each material.

This is illustrated in Fig. 5 that shows the relative deviation between measured and fitted $\Delta P/L$ values [calculated using Eq. (2)] as a function of the measured $\Delta P/L$ for selected

Table 2. Different Approaches and Related Optimal Values of A, B, and a in Terms of Relative Squared Errors for the Three Different Materials

Approach	Equation	A_{granite}	A_{gravel}	A_{Leca}	B_{granite}	B_{gravel}	B_{leca}	a_{granite}	a_{gravel}	a_{Leca}	$\mathrm{RSE}_{\mathrm{granite}}$	$\mathrm{RSE}_{\mathrm{gravel}}$	$\mathrm{RSE}_{\mathrm{Leca}}$	$\mathrm{RSE}_{\mathrm{Tot}}$
Andreasen et al. (2013)	Eq. (2) A, B	481	444	405	53	65	49				0.18	0.17	0.21	0.19
1	Eq. (7) A, B, a	587	604	509	49	63	47	0.72	0.62	0.68	0.15	0.13	0.18	0.15
2	Eq. (7) A, B	599	565	498	49	63	47	0.70	0.15	0.14	0.18	0.16		
3	Eq. (7) A, a	597	642	480	51	0.68	0.15	0.15	0.18	0.16				
4	Eq. (7) B	560	51	63	43	0.73	0.15	0.13	0.18	0.16				
5	Eq. (7) a	560	51	0.73	0.76	0.57	0.15	0.16	0.19	0.17				
6	Eq. (7)	562	51	0.68	0.15	0.17	0.20	0.18						

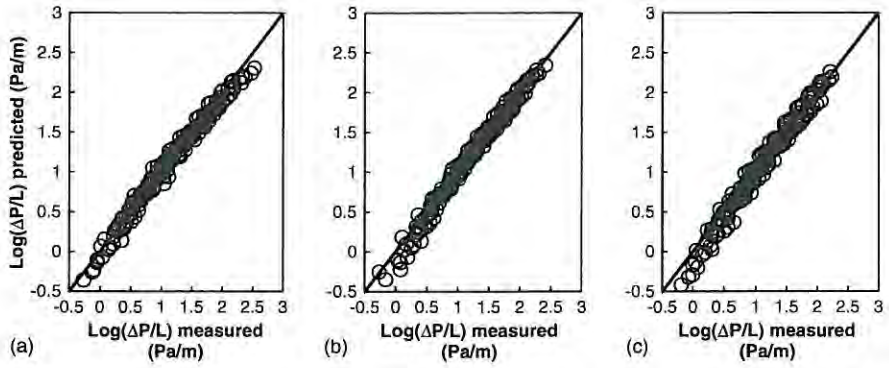

Fig. 4. Fitted [using Eq. (2)] versus measured values of Log $(\Delta P/L)$ for (a) granite; (b) gravel; (c) Leca

particle-size fractions for each of the three materials. In all six cases shown in Fig. 5, the relative deviation between measured and fitted $\Delta P/L$ values as a function of the measured $\Delta P/L$ shows an upward concave relationship. This means that on average the model tends to over predict $\Delta P/L$ at low and high values of $\Delta P/L$ and underpredict at intermediate $\Delta P/L$. This tendency was also observed for all other particle-size fractions across all three materials but tended to be most prominent for particle-size fractions containing mainly small or large particles. The reason is that the model [Eq. (2)] is not able to fully capture the nonlinear relationship between $\Delta P/L$ and V for the materials. As the curvature of the modeled V-$\Delta P/L$ relationship by Eq. (2) is not only controlled by the empirical constants, A and B, but also by the value of D_{eq}, it is likely that a more optimal choice of expression for D_{eq} may improve model results. Andreasen and Poulsen (2013) proposed that D_{eq} might be predicted as the harmonic mean of the smallest and the mean particle diameter present in each particle size fraction [as given by Eq. (1)], thus the smallest and the mean particle sizes are weighted equally in the prediction of D_{eq}. Earlier studies, however, have suggested that the characteristics of granular materials might be predicted using the particle diameters corresponding to the 10 and 60% fractiles of the particle-size distribution, D_{10} and D_{60}, respectively. These particle diameters will also be applicable to nonuniform particle-size distributions while this is not possible when using Eq. (1) as D_{min} is often not known for nonuniform particle-size distributions. Thus, the choice of D_{min} and D_m (corresponding to D_0 and D_{50}) for predicting D_{eq} is likely not the optimal choice. It is also well known that for a given medium consisting of a mixture of particles of different diameters, the smaller particles have a larger impact on $\Delta P/L$ than large particles. Therefore, weighting the two diameters equally in the D_{eq} prediction as done in Eq. (1) may not be the optimal approach.

We, therefore, propose that the following expression for predicting D_{eq} across different materials:

$$D_{eq} = \frac{1}{\left(\frac{a}{D_{10}} + \frac{1-a}{D_{60}}\right)} \tag{6}$$

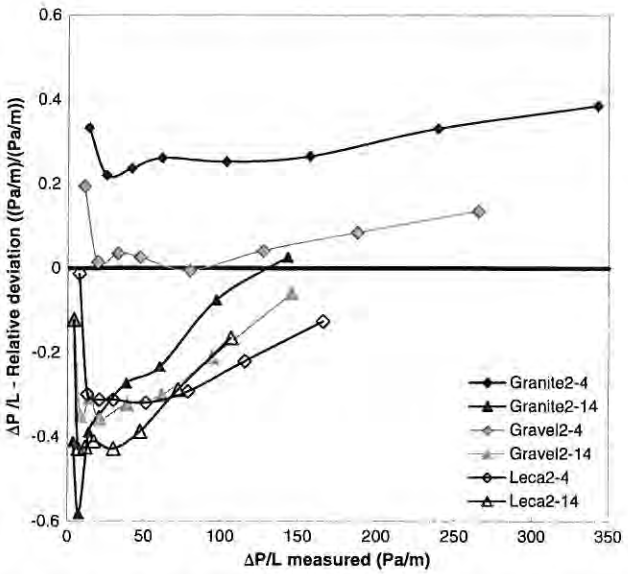

Fig. 5. Relative deviations between fitted [using Eq. (2)] and measured values of $\Delta P/L$ as a function of the measured $\Delta P/L$ for selected particle-size fractions from the three materials considered in this study

where a = a weighting factor $0 < a < 1$; and D_{10} and D_{60} (m) = the particle diameters at which 10 and 60% of the material mass consists of particles with a smaller diameter, respectively. Replacing Eq. (1) with Eq. (6) in Eq. (7) yields

$$\frac{\Delta P}{L} = A\left(\frac{1}{\frac{a}{D_{10}} + \frac{1-a}{D_{60}}}\right)^{-2} \mu V + B\left(\frac{1}{\frac{a}{D_{10}} + \frac{1-a}{D_{60}}}\right)^{-1} \rho V^2 \tag{7}$$

Eq. (7) was, therefore, fitted to the measured V-$\Delta P/L$ data for all three materials using A, B, and a as fitting parameters. Six different fitting approaches were tested: (1) values of A, B, and a were fitted individually for each of the three materials (a total of nine fitting parameters); (2) A and B were fitted individually for each material while one common value of a across all three materials was used (seven fitting parameters); (3) A was fitted individually for each material while common values of B and a were used (five fitting parameters); (4) B was fitted individually for each material while common values of A and a were used (five fitting parameters); (5) a was fitted individually for each material while common values of A and B were used (five fitting parameters); and (6) common values of A, B, and a were used (three fitting parameters). Values of A and B for Eq. (2) and A, B, and a for all six fitting approaches using Eq. (7) are shown in Table 2. Values of the RSE [Eq. (5)] were calculated for each approach both considering each of the three materials individually and all three materials together. These data are also shown in Table 2. Fitted versus measured values of $\Delta P/L$ using approach (1) for all three materials and all gas velocities considered are shown in Fig. 6(a) for granite, Fig. 6(b) for gravel, and Fig. 6(c) for Leca.

The use of Eq. (7) in Approach 1 reduces the RSE by 25% compared to using Eq. (2). The main difference between Eq. (7) in Approach 1 and Eq. (2) is that individual values of D_{eq} for each material are used in the former approach. Thus, although the reduction in RSE is relatively modest, this indicates that improved predictions of $\Delta P/L$ may be achieved by taking into account the effects of particle shape on the value of D_{eq}. Values of A are generally 20–30% higher when using Eq. (7) compared to Eq. (2) while values of B are approximately the same. When using Eq. (7) in Approach 2, there is a clear relationship between A and particle roundness such that A decreases with increasing roundness. For Approaches 1 and 3–6, this tendency is less clear although the lowest values of A are still observed for the highest degree of roundness. Relationships between B, a, and roundness are less clear, although for both parameters the lowest values are observed for the highest degree of roundness indicating that all three parameters A, B, and a are related to particle roundness. Particle roundness may not be the only controlling factor or perhaps not optimal for characterizing particle shape as particles of different shapes may exhibit similar roundness. Also particle characteristics such as surface roughness affect $\Delta P/L$, A, B, and a. Measurement of particle surface roughness on nonspherical particles remains a challenge due to the difficulty in distinguishing particle angularity and particle surface roughness as these two characteristics have similar impact on ΔP.

The data in Table 2, further, show that Eq. (7) can achieve the same (or slightly better) prediction accuracy compared to Eq. (2) using only half the number of empirical fitting parameters [compare Eq. (2) with Eq. (7) Approach 6 in Table 2]. Thus, Eq. (7) offers a much simpler approach for predicting $\Delta P/L$ in granular materials as it only requires one value of A, B, and a regardless of material type, particle shape, and size. The results indicate that $A \approx 562$, $B \approx 51$, and $a \approx 0.7$ are suitable as long as the particle-size distributions of the individual particle-size fractions are uniform. It is very likely that at least some of the empirical parameters A,

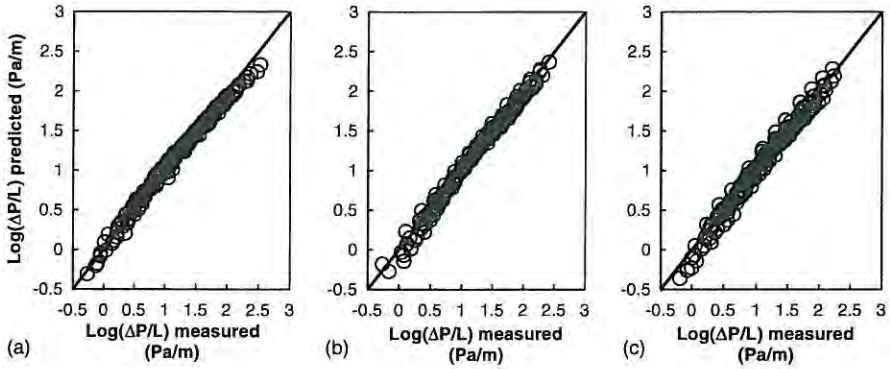

Fig. 6. Measured and predicted [Eq. (7) with A, B, and a fitted individually for each material] values of $\Delta P/L$, for (a) granite; (b) gravel; (c) Leca

B, and a depend on the shape of the particle-size distributions considered, however, more $\Delta P/L$ measurements in media with different particle-size distribution shapes, originating from the same material are needed to verify this.

Conclusions

ΔP as a function of air V was investigated in three different commercially available granular materials, which have very different particle shapes: crushed granite (very angular particles, low roundness); gravel (particles of intermediate roundness); and Leca (almost spherical particles, high roundness). A total of 21 different particle-size fractions were considered, with particle sizes ranging from 2 to 14 mm for each of the three materials.

Overall 1,008 V-$\Delta P/L$ measurements have been carried out. V-$\Delta P/L$ followed a second-order polynomial in agreement with earlier studies. Results showed that $\Delta P/L$ decreased with increasing particle size and that it was inversely correlated with active air-filled porosity. The latter is in contrast to earlier findings for fine-grained materials such as soils and is likely because the pore structure for fine-grained materials is very different from coarse-granular materials used here. Values of $\Delta P/L$ generally decreased with particle roundness. For granite and gravel, $\Delta P/L$ was 1.24 and 1.19 times larger than for Leca on average. Differences in $\Delta P/L$ between the three materials were most prominent for the fractions containing smaller particles. This supports the hypothesis that at least part of the differences in ΔP observed between the three materials used here stems from differences in particle shape (roundness).

An existing model for predicting $\Delta P/L$ as a function of V, developed for Leca, was tested against the V-$\Delta P/L$ values measured in this study, for all three materials. The model performed relatively well although it had a tendency to underpredict small and large while overpredicting intermediate $\Delta P/L$ values. This was the case for the three data sets as a whole but also for the individual particle-size fractions for each material. Thus, an improved model for predicting the V-$\Delta P/L$ relationship was proposed.

This model was able to yield the same accuracy of V-$\Delta P/L$ predictions as the existing model using only half the number of model-fitting parameters (three instead of six) and is, thus, simpler to apply. Results from the modeling further indicated that the material-specific empirical parameters were related to particle shape. Further measurements on other materials with a wider range of particle-size distribution and particle shapes, however, are required to better understand the relationship between the V-$\Delta P/L$ relationship for a given material and its particle size distribution, particle shape, and other characteristics such as particle surface roughness.

References

Ahmed, N., and Sunada, D. (1969). "Nonlinear flow in porous media." *J. Hydr. Div.*, 95(6), 1847–1857.

Andreasen, R. R., Canga, E., Kjaergaard, C., Iversen, B. V., and Poulsen, T. G. (2013). "Relating water and air flow characteristics in coarse granular materials." *Water Air Soil Pollut.*, 224(4).

Andreasen, R. R., Nicolai, R. E., and Poulsen, T. G. (2012). "Pressure drop in biofilters as related to dust and biomass accumulation." *J. Chem. Technol. Biotechnol.*, 87(6), 806–816.

Andreasen, R. R., and Poulsen, T. G. (2013). "Air flow characteristics in granular biofilter media." *J. Environ. Eng.*, 10.1061/(ASCE)EE.1943-7870.0000640, 196–204.

Antohe, B. V., Lage, J. L., Price, D. C., and Weber, R. M. (1997). "Experimental determination of permeability and inertia coefficients of mechanically compressed aluminum porous matrices." *J. Fluids Eng.*, 119(2), 404–412.

Barona, A., Elias, A., Arias, R., Cano, I., and Gonzales, R. (2004). "Biofilter response to gradual and sudden variations in operating conditions." *Biochem. Eng. J.*, 22(1), 25–31.

Barret, P. J. (1980). "The shape of rock particles, a critical review." *Sedimentology*, 27(3), 291–303.

Bowman, E. T., Soga, K., and Drummnond, W. (2001). "Particle shape characterisation using Fourier descriptor analysis." *Geotechnique*, 51(6), 545–554.

Carman, P. C. (1937). "Fluid flow through granular beds." *Trans. Inst. Chem. Eng.*, 15, 150–166.

Chin, D. A., Price, R. M., and DiFrenna, V. J. (2009). "Nonlinear flow in karst formations." *Ground Water*, 47(5), 669–674.

Connell, H., Zhu, J., and Bassi, A. (1999). "Effect of particle shape on crossflow filtration flux." *J. Membr. Sci.*, 153(1), 121–139.

Cornell, D., and Katz, D. L. (1953). "Flow of gases through consolidated porous media." *Ind. Eng. Chem.*, 45(10), 2145–2152.

Cox, E. P. (1927). "A method of assigning numerical and percentage values to the degree of roundness of sand grains." *J. Paleontol.*, 1(3), 179–183.

Darcy, H. (1856). *Les fontaines publiques de la ville de dijon*, V. Dalmont, ed., Paris.

De Oliveira, L. L., Duarte, I. C. S., Sakamoto, I. K., and Varesche, M. B. A. (2009). "Influence of support material on the immobilization of biomass for the degradation of linear alkylbenzene sulfonate in anaerobic reactors." *J. Environ. Manage.*, 90(2), 1261–1268.

Elias, A., Arias, R., Cano, I., Gonzales, R., and Barona, A. (2003). "Effect of sudden variations in operating conditions on biofilter performance." *Air Pollut.*, 13, 523–529.

Endo, Y., Chen, D. R., and Pui, D. Y. H. (2001). "Air and water permeation resistance across dust cakes on filters-effects of particle polydispersity and shape factor." *Powder Technol.*, 118(1–2), 24–31.

Ergun, S. (1952). "Fluid flow through packed columns." *Chem. Eng. Prog.*, 48(2), 89–94.
Fair, G. M., and Hatch, L. P. (1933). "Fundamental factors governing the streamline flow of water through sand." *J. — Am Water Works Assoc.*, 25, 1551–1565.
Forchheimer, P. H. (1901). "Wasserbewegung durch boden." Zeitschrift ver deutscher ingenieure 50, 1782–1788 (in German).
Gadal-Mawart, A., Malhautier, L., Renner, C., and Fanlo, J. L. (2010). "Physicochemical and hydrodynamic characterisation of various packing materials for biofiltration." *Proc., 2010 Duke-UAM Conf. on Biofiltration for Air Pollution Control*, Duke Univ., Durham, NC.
Geertsma, J. (1974). "Estimating coefficient of inertial resistance in fluid-flow through porous-media." *Soc. Pet. Eng. J.*, 14(5), 445–450.
Goldstein, N. (1996). "Odor control experiences: Lessons from the biofilter." *Biocycle*, 37(4), 70–74.
Green, L., and Duwez, P. (1951). "Fluid flow through porous metals." *J. Appl. Mech. Trans. ASME*, 18(1), 39–45.
Hamamoto, S., Moldrup, P., Kawamoto, K., and Komatsu, T. (2009). "Effect of particle size and soil compaction on gas transport parameters in variably saturated, sandy soils." *Vadose Zone J.*, 8(4), 986–995.
Hausrath, E. M., Neaman, A., and Brantley, S. L. (2009). "Elemental release rates from dissolving basalt and granite with and without organic ligands." *Am. J. Sci.*, 309(8), 633–660.
Kim, N. J., Hirai, M., and Shoda, M. (2000). "Comparison of organic and inorganic packing materials in the removal of ammonia gas in biofilters." *J. Hazard. Mater.*, 72(1), 77–90.
Kozeny, J. (1927). "Über kapillare leitung des wassers im boden." *Akad. Wiss. Wien*, 136, 271–306 (in German).
Krumbein, W. C. (1941). "Measurements and geological significance of shape and roundness of sedimentary particles." *J. Sediment. Petrol.*, 11(2), 64–72.
Lage, J. L., Antohe, B. V., and Nield, D. A. (1997). "Two types of nonlinear pressure-drop versus flow rate relation observed for saturated porous media." *J. Fluids Eng. Trans. ASME*, 119(3), 700–706.
Macdonald, I. F., El-Sayed, M. S., Mow, K., and Dullien, F. A. L. (1979). "Flow through porous media—The Ergun equation revisited." *Ind. Eng. Chem. Fundam.*, 18(3), 199–208.
Macdonald, M. J., Chu, C. F., Guilloit, P. P., and Ng, K. M. (1991). "A generalized Blake-Kozeny equation for multisized spherical-particles." *Aiche J.*, 37(10), 1583–1588.
Malhautier, L., Khammar, N., Bayle, S., and Fanlo, J. L. (2005). "Biofiltration of volatile organic compounds." *Appl. Microbiol. Biotechnol.*, 68(1), 16–22.
McNevin, D., and Barford, J. (1998). "Modelling adsorption and biological degradation of nutrients on peat." *Biochem. Eng. J.*, 2(3), 217–228.
Meloy, T. P. (1977). "Fast Fourier transforms applied to shape analysis of particle silhouettes to obtain morphological data." *Powder Technol.*, 17(1), 27–35.
Nicolai, R. E., and Janni, K. A. (2000). "Designing biofilters for livestock facilities." *Proc. 2nd Int. Conf. on Air Pollution from Agricultural Operations*, American Society of Agricultural Engineers, St. Joseph, MI, 376–383.
Omosanya, K. O., Mosuro, G. O., Laniyan, T. A., and Ogunleye, D. (2012). "Prediction of gravity anomaly from calculated densities of rocks." *Adv. Appl. Sci. Res.*, 3(4), 2059–2068.
Pentland, A. (1927). "A method of measuring the angularity of sands." *Royal Soc. Canada Proc. Trans.*, 21(3), Appendix C.
Pugliese, L., Poulsen, T. G., and Andreasen, R. R. (2012). "Relating gas dispersion in porous media to medium tortuosity and anisotropy ratio." *Water Air Soil Pollut.*, 223(7), 4101–4118.
Rouse, P. C., Fannin, R. J., and Shuttle, D. A. (2008). "Influence of roundness on the void ratio and strength of uniform sand." *Geotechnique*, 58(3), 227–231.
Sakuma, T., Hattori, T., and Deshusses, M. A. (2006). "Comparison of different packing materials for the biofiltration of airtoxics." *J. Air Waste Manage. Assoc.*, 56(11), 1567–1575.
Santamarina, J. C., and Cho, G. C. (2004). "Soil behaviour: The role of particle shape." *Proc., Skempton Conf.*, British Geotechnical Association, Imperial College London, London.
Scheidegger, A. E. (1960). *The physics of flow through porous media*, Macmillan, New York.
Sharma, P., and Poulsen, T. G. (2010). "Gas dispersion and immobile gas volume in solid and porous particle biofilter materials at low air flow velocities." *J. Air Waste Manage. Assoc.*, 60(7), 830–837.
Shinohara, K., Oida, M., and Golman, B. (2000). "Effect of particle shape on angle of internal friction by triaxial compression test." *Powder Technol.*, 107(1–2), 131–136.
Sorrentino, J. A., and Anlauf, H. (1999). "Some simple relationships about the influence of particle size distribution on cake permeability." *Adv. Filtrat. Separ. Technol.*, 13A–13B, 917–925.
Sperl, J., and Trckova, J. (2008). "Permeability and porosity of rocks and their relationship based on laboratory testing." *Acta Geodyn. Geomater.*, 5(1), 41–47.
Tickell, F. G. (1931). *The examination of fragmental rocks*, Stanford University Press, London.
Trussell, R. R., and Chang, M. (1999). "Review of flow through porous media as applied to head loss in water filters." *J. Environ. Eng.*, 10.1061/(ASCE)0733-9372(1999)125:11(998), 998–1006.
Wadell, H. (1935). "Volume, shape and roundness of quartz particles." *J. Geol.*, 43(3), 250–280.
Wani, A. H., Branion, R. M. R., and Lau, A. K. (1997). "Biofiltration: A promising and cost-effective control technology for odors, VOCs and air toxics." *J. Environ. Sci. Health Part A: Toxic/Hazard. Subst. Environ. Eng.*, 32(7), 2027–2055.
Ward, J. C. (1966). "Closure to turbulent flow in porous media." *J. Hydr. Div.*, 92(4), 110–121.
Witt, K. J., and Brauns, J. (1983). "Permeability—anisotropy due to particle shape." *J. Geotech. Eng.*, 109(9), 1181–1187.